nature reviews electrical engineering

https://doi.org/10.1038/s44287-024-00061-6

Review article

Check for updates

Triboelectric nanogenerators for wind energy harvesting

Md Al Mahadi Hasan [1,2,6], **Wenxuan Zhu** [1,3,6], **Chris R. Bowen** [4], **Zhong Lin Wang** [1,5] ✉ & **Ya Yang** [1,2,3] ✉

Abstract

Researchers in different disciplines from all around the world are constantly working on the development of new technologies for harvesting energy from sustainable sources. Among the various alternatives, wind is one of the most abundant resources. Traditionally, wind energy has been harvested to produce electrical energy using various types of wind turbines, including onshore or offshore wind turbines, horizontal or vertical axis wind turbines and micro-wind turbines; or, less traditionally, using wind pumps, or windmills, on sailing boats, and through some sports activities (such as kiteboarding, windsurfing and kitesurfing). In this context, wind energy harvesting using triboelectric nanogenerators (TENGs) has unique characteristics able to challenge the existing wind energy harvesting technologies. Wind-driven TENGs are in fact characterized by simple structures, reduced size and weight, easy installation, flexibility and low-cost operation. Here, starting from a detailed comparison with conventional wind turbine systems, we introduce the technological advancement of wind-driven TENGs. Device structures, materials, fabrication processes and performance characteristics in terms of costs and applications are outlined. Open issues and challenges to be addressed towards the development and industrialization of commercial products are also presented.

Sections

[1]Beijing Key Laboratory of Micro-Nano Energy and Sensor, Center for High-Entropy Energy and Systems, Beijing Institute of Nanoenergy and Nanosystems, Chinese Academy of Sciences, Beijing, China. [2]School of Nanoscience and Technology, University of Chinese Academy of Sciences, Beijing, China. [3]School of Chemistry and Chemical Engineering, Center on Nanoenergy Research, Guangxi University, Nanning, Guangxi, China. [4]Department of Mechanical Engineering, University of Bath, Bath, UK. [5]School of Materials Science and Engineering, Georgia Institute of Technology, Atlanta, GA, USA. [6]These authors contributed equally: Md Al Mahadi Hasan, Wenxuan Zhu. ✉e-mail: zhong.wang@mse.gatech.edu; yayang@binn.cas.cn

Key points

• Wind-driven triboelectric nanogenerators (W-TENGs) can be used to harvest energy from low-speed and high-speed omnidirectional winds with notable power density.

• W-TENG-based energy harvesting technology overcomes challenges associated with conventional methods such as structural constraints, structural complexity, large volume, expensive installation, low efficiency and irregular wind speed environments.

• The possibility of hybridization with different technologies makes W-TENGs suitable to be deployed in decentralized sensor applications, such as smart agriculture or the internet of things.

• The potential application of W-TENGs in portable electronics, smart home appliances, smart cities, air cleaning and industrial monitoring systems opens the way to industrialization.

Introduction

In response to the global energy crisis, finding alternative ways for electricity production, moving away from traditional energy sources, is paramount[1]. The world-wide production of electricity still largely depends on fossil fuels (60%) and the energy demand is projected to increase three times by 2050 (ref. 2). In this context, wind energy harvesting has received notable attention because of its clean and renewable resources[3–7]. According to the latest report by the Global Wind Energy Council, the total installed wind energy capacity will be around 2 TW by the end of 2030 (ref. 8).

First introduced in the late nineteenth century, wind turbine-based plants for wind energy harvesting had a rapid development in the 1980s (refs. 6,9,10). Wind turbine technology converts the mechanical energy of the wind into electrical energy, through the rotation of rotor blades, which is the driving force for the generator[9,11]. The efficiency in energy harvesting of wind turbines primarily depends on their specific locations and on the meteorological conditions (speed and direction of the wind)[12,13]. Conventional wind turbines (Fig. 1a) comprise several rotating parts (rotor blades, blade pitch controllers, generators, gearboxes and yaw control) and supporting components (rotor hubs, brakes, high towers, access ladders and heavy basements). Because of their bulky structures, wind turbines present several challenges, such as complex design, large volume, heavy weight, high installation cost, low efficiency and considerable losses in power transmission from isolated locations[9,14–19].

Triboelectric nanogenerator (TENG) technology is a promising alternative for wind energy harvesting[20,21]. TENGs were introduced in 2012 as a new way of harvesting mechanical energy from environmental sources that are commonly wasted, such as human activities, rotating tyres, ocean waves and many more[20]. Wind-driven TENGs (W-TENGs) use alternative wind sources, such as low-speed wind or wind generated by high-speed vehicles[22–24]. W-TENGs are expected to be widely used in the future for wind power collection owing to the large range of employable wind speeds, the possibility of harvesting omnidirectional wind and the relatively high-power density[25–33]. Since their introduction, W-TENGs have increased their power generation from some microwatts to around 20 mW and demonstrated the ability of exploiting winds at extremely low speeds such as 0.2 m s^{-1} (refs. 25,32). W-TENGs are characterized by simple structures, reduced size and weight, easy installation, flexibility and low-cost operation[34–39]. They offer excellent design flexibility for their simple structures (Fig. 1b), which only include two electrodes and a dielectric layer as functional materials and substrates and bolts as the supporting bodies of the devices[39,40]. This emerging energy harvesting technology can be integrated and hybridized with other energy harvesting techniques[41–49] and it can be deployed in decentralized sensor applications[50], in smart agriculture[46,47] or for the internet of things (IoT)[51], enabling the operation of sensor networks in adverse weather conditions and restricted areas[36,52].

In this Review, we evaluate the state of the art of W-TENGs and their potential as wind energy harvesting systems. We start with a detailed comparison between W-TENGs and conventional wind turbines. We then describe the various W-TENG device architectures, their working principles and their performance. We discuss the strengths and the weaknesses of the different applications of W-TENGs. Furthermore, we address cost analysis and performance influencing factors and introduce alternative approaches to enhance the performance. Finally, we outline the status of W-TENG applications towards industrialization.

Comparison between W-TENGs and conventional wind turbines for energy harvesting

The interest in W-TENGs has risen from the necessity of overcoming critical challenges posed by conventional wind turbines, such as complexity in installation and high cost. To compare W-TENGs and conventional wind turbines, three main aspects should be considered (Table 1): working principles (Box 1), characteristics (in terms of size, weight, lifetime, fabrication requirements and so on) and applications.

Conventional wind turbines generally have large components with high mass and lifting complexity (for example, blades and towers can be at several hundreds of metres from the ground level) that require the employment of heavy machinery during the installation processes. In the early 1980s, turbine diameters were between 10 m and 20 m (ref. 53). Forty years later, they have now crossed the three digits range (up to 236 m)[1]. Typical dimensions of W-TENGs are from a few centimetres to around a metre[1,40,54]. Likewise, the weight of conventional wind turbines reaches several hundreds of tons, whereas W-TENGs are in the single digits of kilograms[35,52,55,56].

W-TENGs are easier to implement than conventional wind turbines because they do not have any structural constraints (such as rotating components), operating mechanism (their working principle depends only on the friction between two different materials) or fabrication and maintenance cost complexity[57] (for example, the absence of rotating parts eliminates the need for expensive lubricants and difficult maintenance operations, see Box 2). Conventional wind turbines need massive construction sites with heavy machinery supports during the installation time and during replacing or translocating, which are not necessarily so complex or time-consuming in the case of W-TENGs. Moreover, owing to their light weight and flexibility, W-TENGs can be installed with low complexity and low cost on already existing systems or independently.

Conventional wind turbines necessitate one-directional winds and specific wind speeds (which are calculated considering the tower height, blade length, generator capability, transformer capacity, and are typically in the range of 5–35 m s^{-1})[58], whereas W-TENGs have less stringent speed limits (from around 0.2 m s^{-1} to higher than 80 m s^{-1})[25,26] and can effectively harvest omnidirectional winds[27,59,60]. For these reasons, W-TENG-based technology makes an excellent choice for areas where the employment of conventional harvesters is difficult, such as broadband energy[47,61,62], gentle breeze[29,46,49,55,63–66], human motion[67–69], high-speed train[26] and highway wind[22].

From the perspective of the applications, W-TENGs can be deployed in densely populated areas as portable power supply for smaller electronic devices, environmental monitoring and sensor networks because they do not require open or flat space for operation[70–72]. Moreover, W-TENGs do not have safety issues. Conventional wind turbines generate a certain amount of noise during operation, and the rotation of the blades can lead to bird deaths, impacting the ecosystem and the environment[1,14].

When considering the lifetime and the power output performance, conventional wind turbines are far ahead. However, in the early 2020s, W-TENGs have shown notable improvements in this sense, owing to new materials and boosting strategies[31,32,73]. For example, a fluttering W-TENG with a power output peak of 38.16 mW at a wind velocity of 6 m s^{-1} was reported in 2023 (ref. 31). In 2022, the lifetime of a W-TENG was improved owing to the introduction of new materials (polyvinyl chloride/MoS_2 composite); a steady output current signal was recorded under continuous working conditions for 15 h (ref. 73).

Overall, in comparison with conventional wind turbines, W-TENGs are preferable in terms of size, cost, flexibility, applications and safety when dealing with emergencies or to be used in densely populated regions. As a result, the potential of the W-TENG in distributed sensor networks has no rival to compete in such circumstances. Further research in the field can expand the areas of application. For example, they can be used as an alternative power supply to traditional lithium-based batteries in which waste materials are an alarming issue for environmental safety.

Structures and materials of W-TENGs

W-TENGs have simple structures owing to the simplicity of their working mechanism, which is solely based on the contact between two surfaces. In most cases, the working principle is the main criterion that defines the specific structure. Besides the mechanism-based choice of the structure, W-TENGs can be easily modified according to the wind energy source that needs to be harvested or to the final application. New materials and structures are evolving very fast to enhance the device performance and expand the application areas. Environmental conditions such as wind speed, humidity and temperature are also important factors in choosing appropriate materials and structures. In general, the higher the wind speed, the higher the power output[54,55,74]; the lower the temperature and humidity, the better the power output[37,75]. Although some external conditions can be controlled, others such as cyclones, extreme rain and irregular wind orientation cannot be controlled; therefore, it is important to consider the possible effects of these external conditions when designing the device and choosing the materials and the structures.

Structures

The architecture of W-TENGs depends on the working principle of the employed TENG. TENGs are characterized by four main working modes: contact-separation mode[40], horizontal sliding mode[76], single electrode mode[77] and separate layer mode[78]. The majority of the W-TENGs reported in the literature are based on contact separation mode or on horizontal sliding mode. The choice of the working principle is mainly related to the environmental conditions of the application. W-TENGs present four architectures: (1) both-end fixed W-TENGs based on contact separation mode[36] (Fig. 2a); (2) single-end fixed W-TENGs based on contact separation mode[40] (Fig. 2b); (3) flag-type W-TENGs[77,79] (Fig. 2c);

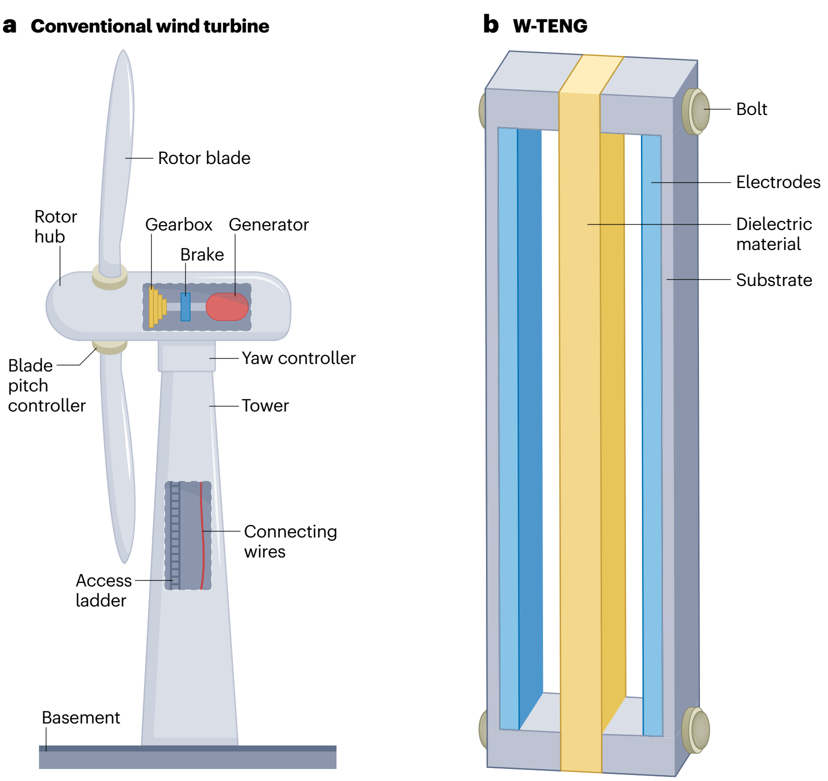

Fig. 1 | Schematic structure of a conventional wind turbine and a wind-driven triboelectric nanogenerator. a, Schematic architectural view of a wind turbine energy harvesting system with its fundamental structural and functional components. **b**, Schematic structure of a wind-driven triboelectric nanogenerator (W-TENG).

Table 1 | Comparison between conventional wind turbines and wind-driven triboelectric nanogenerators

		Conventional wind turbines	Wind-driven triboelectric nanogenerators
Working mechanism		Faraday's electromagnetic induction	Contact electrification and electrostatic induction
Scope	Wind energy source	Natural wind	Natural wind, human motion, subways and high-speed rails
	Location dependency	Location-oriented	Not location oriented
Characteristics	Size[1,26]	Up to 236 m	Up to 1 m
	Lifetime[147]	Up to 25 years	Several months
	Weight	Heavily weighted	Extremely light
	Cost[57]	Extremely expensive	Very cheap
	Wind speed range[25,58,147]	5–35 $m s^{-1}$	0.2–82 $m s^{-1}$
	Output power[25,57]	Up to 12 MW	V_{oc} = 2,000 V, I_{sc} = 4 A
Related issues	Environmental factors[14]	Noisy, dangerous for animals, high risk of accidents	Less noisy, no danger for animals and risk-free of accidents
	Application areas	Energy harvesting	Energy harvesting, environmental monitoring and distributed sensors
	Portability	No portability	Excellent portability
	Flexibility (installation, location and maintenance)	Low	High
Other factors	Housing space	Large (device and related equipment)	Small (device only)
	Machinery requirement	High-weight equipped system	Low-weight equipped system
	Expertise	Need a high-level trained team for the operation	Need a lightly trained team for the operation
	Integration flexibility[148]	Individual installation for safety reasons	Possibility of having device arrays

I_{sc}, short circuit current; V_{oc}, open circuit voltage.

and (4) turntable-type W-TENG[46,80] (Fig. 2d). To describe the different possible W-TENG structures, fluorinated ethylene propylene (FEP) (for the dielectric material) and Cu and Al (for the electrodes) have been considered as reference materials as they are the most employed materials in W-TENGs fabrication. In the both-end fixed W-TENG, the functional layer of the FEP film is fixed at both ends in a sandwich-like structure between two aluminium foils, which work as electrodes. When air flows across the structure, the airflow drives the FEP film to either the top or the bottom aluminium electrodes, charging the surfaces. In this case, the vibration of the FEP film is a result of Karman vortex shedding[39,81]. As the FEP film moves up and down under the action of the wind flow, through the electrostatic induction effect, the charge is transferred between the two electrodes, producing an alternating current whose direction is indicated in Fig. 2a. This type of structure can work with high-speed winds. Good structural stability can be obtained if heavy metallic electrodes (such as Al bars) are employed as the supporting body of the W-TENG[82].

The single-end fixed and the flag-type structures have a similar working principle, in which one side of the FEP film is kept free to move (Fig. 2b,c). For the type 2 structure, only the FEP layer is movable, whereas in the case of type 3, the whole sandwich can move following the frequency of the wind vortex from any direction. The specific oscillation frequency generated by the wind is the driving force of these devices. Thus, they can harvest energy from very-low-speed winds (0.2 $m s^{-1}$) but with low and unstable outputs[23,25].

The turntable-type structure is characterized by a completely different structure of circular shape (Fig. 2d): a copper plate is added at the top of the device[83]. In this structure, external rotating blades, such as the ones employed in wind turbines, are responsible for the W-TENG operation. The triboelectric layers and the electrodes rotate with the help of external blades, and the frictional contact between the electrode and the dielectric layer causes contact electrification. Novel structures are being developed based on this type of structure. The centrifugal brake structure, for example, contains a stator and a rotator that work with the wind flow through ventilators[84].

The collection of wind energy with the different structures of W-TENGs directly affects the functional surfaces (dielectric layers and electrodes), leading to changes in the contact area. Variation in charge transfer occurs; angle-shaped W-TENG is designed in which two Al electrodes make an angle with an FEP film, which can completely touch surfaces of both electrodes, thus increasing the contact area in comparison to the normal sandwiched single-end fixed structure[55,63,85].

In addition, new W-TENG structures are continuously investigated to optimize the device performance. For example, the parallel double-end fixed-type structure can be modified into an arch-shaped structure to increase the contact area of the W-TENGs and to enhance its performance[23]. In addition to structural optimization, the external component of the W-TENG is also an important factor; an external anemometer TENG part is used for collecting wind energy[72] connected to the main W-TENG section, and an approach to deploy an external channel to collect wind energy and to increase the air speed has been reported[55]. Circuit management methods such as multiplier circuits influence the device output[74,86,87]. Some strategies such as decreasing the thickness of the dielectric film and using capacitors and charge pumping by deploying voltage booster circuits are used to increase the surface charge density of W-TENGs[31,88].

In terms of applications, the first three structures are mainly deployed with directional winds of different speeds[40,89]. The fourth structure is used in omnidirectional wind harvesting[60,90]. The flag-type structure can also be employed with omnidirectional wind but with low performance[75,78,79]. In many cases, the most challenging aspect is the stability of the device, especially for those devices able to harvest omnidirectional winds with fast changes in wind speeds[36,90].

Materials

Surface charge density, surface roughness and surface water resistance are the physical properties that mostly influence the selection of the materials[91,92]. Several methods can be used to enhance the surface charge density: modifying the crystallinity of the materials, injecting extra charges into the devices or introducing functional groups or defects[39,76]. Chemical etching, plasma etching and 3D printing have been deployed to improve the surface roughness and, consequently, to increase the device efficiency[52,70,74,93]. In addition, the polarity, hydrophobicity, transparency, durability and flexibility of the materials influence the device performance[94–98].

Polymers such as FEP, polyvinylidene fluoride, nylon, polyethylene terephthalate and polyamide are the most used dielectric layers, characterized by good hydrophobicity, transparency and excellent triboelectric properties. Al and Cu are often used as electrodes for their high toughness and strength, fundamental properties for making W-TENG structures long-lasting and stable in operation[42,52,67,92,99,100].

Being a relatively new technology, the range of employed materials is growing rapidly. As the research field progresses, new materials are being constantly investigated to improve the surface charge density and device sustainability[67,100]. For example, leaf-based and biomaterials-based devices have been demonstrated[25,82]. Functionalized polyacrylonitrile nanofibres[94] and organic semiconductors, such as poly(3,4-ethylenedioxythiophene)-poly(styrenesulfonate)[100], have been investigated to increase the surface charge density. Carbon materials such as methyl-graphdiyne and polylactic acid have been deployed with some excellent applications in smart agriculture[46,76,101].

Box 1 | Working principles of conventional wind turbines and wind-driven triboelectric nanogenerators

An alternating current generator — based on Faraday's law of electromagnetic induction — is the core component of conventional wind turbines. An electromotive force is produced when an electric conductor is rotated in a static magnetic field (see the figure, panel **a**), or by rotating a magnetic field around a stationary electric conductor[43,45,149]. In wind turbines, the rotation of the conductor shaft, connected to the rotor blades, caused by the vortex force of the wind leads to a change in the magnetic field, thereby generating an electric potential and an electric current in the circuit[150,151].

Contact electrification is the displacement of surface charges caused by the different attraction for electrons when two materials are put into contact. The triboelectric effect — the working principle of triboelectric nanogenerators — is the transfer of electric charge that happens when two materials come into frictional contact with each other. The electron transfer between two materials depends on their rank in the triboelectric series, which is a series of materials according to their tendency to gain or lose electrons. The most positive triboelectric material (the tribopositive layer) loses electrons and becomes positively charged, whereas the most negative triboelectric material (the tribonegative layer) gains electrons and becomes negatively charged[71,152]. When the device is in its original position, there is no charge movement (see the figure, panel **b**). A frictional charge is generated only when the dielectric layer gets into contact with the bottom electrode. When they begin to separate, a difference in the electric potential is produced and the positive charge moves from the bottom electrode to the top one. Again, although the surfaces are moving close to the top electrode, positive charges will be flowing toward the bottom electrode from the top electrode, through the external circuit. An electrostatic induction is a result of the redistribution of charges by attraction and repulsion under an electric field. The combination of these two effects allows for a constant transfer of charge through an external circuit, thereby generating an electric current[153].

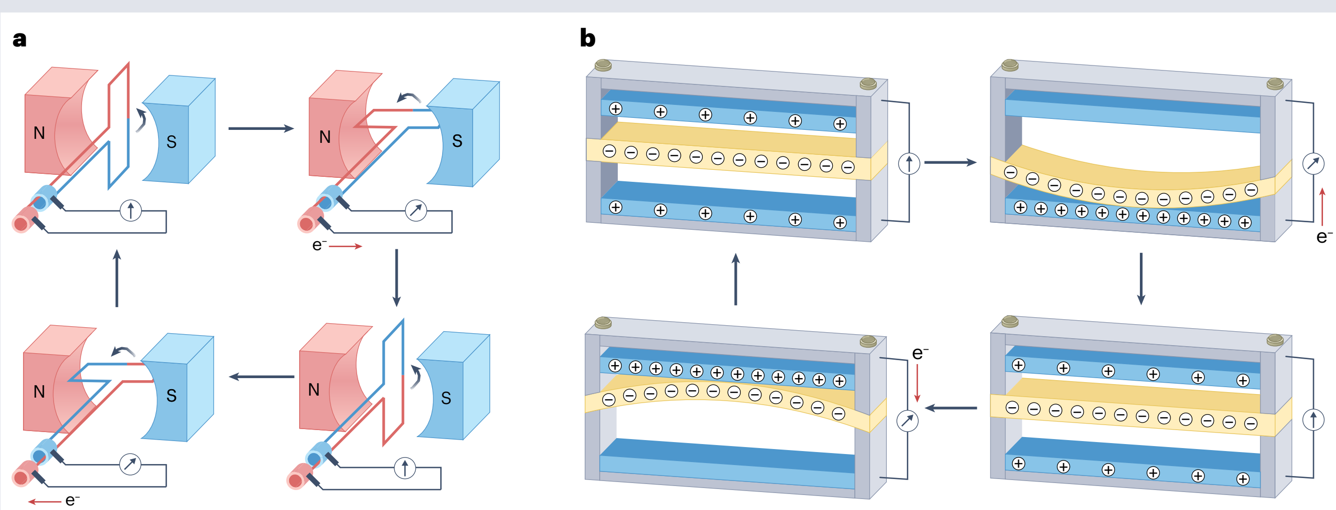

Box 2 | Comparative cost analysis between wind-driven triboelectric nanogenerators and conventional wind turbines

Levelized cost of energy (LCOE) is a parameter used to describe the average net cost of production per energy unit over the lifetime of the energy harvester. LCOE is one of the major issues for most conventional sustainable energy resources and of concern for less-developed countries in the attempt to fight global warming and other environmental problems. Wind-driven triboelectric nanogenerator (W-TENG) technology offers a valid alternative to conventional wind turbines as a low-cost energy harvesting approach[31,57]. As a reference for W-TENGs, we have chosen a study published in 2023 in which a charge excitation mechanism is introduced to boost the device performance[31]. In this work, the output power from a single device is around 38.2 mW. The proposed W-TENG requires a small amount of electrodes, materials and other equipment that reduces the LCOE cost compared with other technologies. For the cost analysis process, we have considered the cost of the materials used to fabricate a single device. A total amount of around US$1.6 (see the figure, panel **a**) includes the cost of the acrylic sheet, the Al tape, the Kapton tape, the high-voltage diodes, the capacitors, the fluttering sheet, the installation cost, the operational cost and other costs related to the operation and the maintenance of the device (miscellaneous). We have collected the reference price from the online shopping merchant Alibaba, which is convenient for the actual fabrication cost calculation.

To compare our reference W-TENGs with conventional wind turbines, the LCOE values for 1 MW were calculated using the following equation:

$$\text{LCOE} = \frac{\text{Total costs over lifetime of the device}}{\text{Total electrical energy produced over lifetime of the device}} \quad (1)$$

The LCOE of the conventional turbines has been collected from the assessment report of 2022 by the National Renewable Energy Laboratory[57]. To generate 1 MW energy with a power output of 38.16 mW, 17,996 devices are needed, making a total cost of US$36,000 if we consider US$2.00 per device. Here, our analysis of the cost–effectiveness includes the cost of device integration as we need a massive number of devices to be connected altogether to get such a high power output. The cost of integration per W-TENG device is considered US$0.05, which is far more than the requirement because most of the time the installation of these devices is attached to some existing site, such as the anti-glare panel arrays on highways, that needs no installation cost or the serially stacked devices without having more complexity to stack up a lot of devices together[22]. Serially stacked W-TENGs generated an adequate amount of power for 12 hygrometers and 3,000 LEDs, which is inspiring for the feasibility of large-scale integration of W-TENGs[32]. Considering a lifetime of 5 months, the LCOE of the W-TENG becomes only US$10, which is the lowest value when compared with conventional wind turbines (see the figure, panel **b**), making the potential of these devices for mass production of energy evident. Even considering a lifetime for the W-TENGs of 1 year (a shorter period if compared with other technologies), the LCOE less than US$5 makes this technology a feasible alternative for energy harvesting (also considering that further research on device integration and stability enhancement could lower the cost even further).

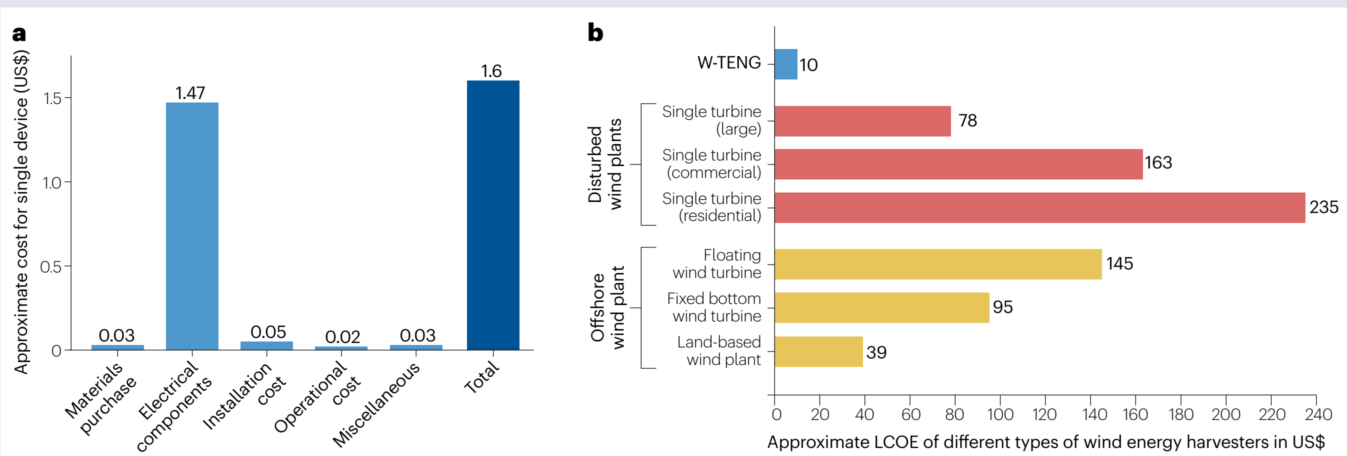

The first single-end W-TENG, proposed in 2013, comprised aluminium foils as the top and bottom electrodes with an FEP film fixed between them as the triboelectric material[40]. A double-end W-TENG was implemented in 2015 to provide better stability to the structure[36]. To this aim and to prolong the lifetime of the devices, additional structures such as the simple flag type, the flutter type, the complex centrifugal brake and other structures with rotating triboelectric layers have then been investigated[65,79,84,102]. A certain number of W-TENGs are serially stacked to create an ionizing channel that polarizes electrodes with charges and creates a higher output in the discharging cycle[32].

For energy-scavenging devices, stable power outputs and lifetimes are highly important. The stable operation has been demonstrated up to more than 1,400,000 cycles, making applications, such as smart farming[103], wind speed monitoring[89] and anti-glare panel arrays in highways[22], possible. Besides, the polymers commonly used for W-TENGs are stable both in ultra-low (0.2 m s^{-1}) and extremely high (80 m s^{-1})

speeds, making the devices usable for long periods (up to several months)[25,40]. In addition, with the ongoing research on alternative materials synthesis and biodegradable or biomaterials use, these devices are becoming greener energy sources with excellent stability in device operation[25,50,73,104]. Complex centrifugal brake-type structures or leaf-like structures (with the use of textile polymers) have been introduced to increase flexibility and to decrease cost[25,67,77,82,84].

Performance of W-TENGs

W-TENG-based energy harvesting has become an active multidisciplinary research field starting from the initial years of the 2010s, with continuous improvements in the performance and number of applications over the years.

The metrics to evaluate the performances of a W-TENG device, and consequently define its suitability for a specific application, are

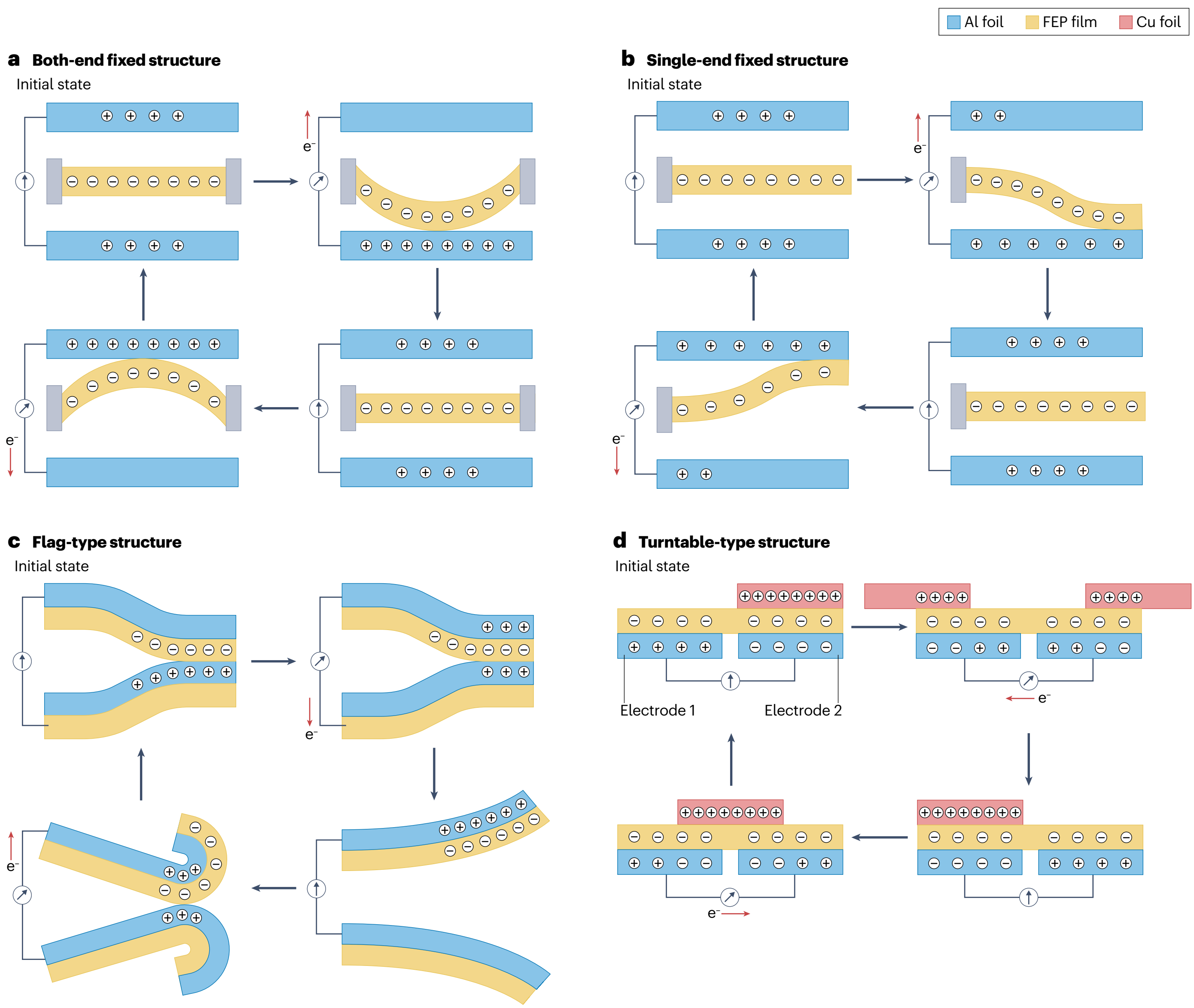

Fig. 2 | Working principle of a single cycle for the different structures of wind-driven triboelectric nanogenerators. a, Both-end fixed structure. **b**, Single-end fixed structure. **c**, Flag-type structure. For the structures reported in panels **a**–**c**, in the initial state, the electrodes (indicated here as Al foil) and the dielectric film (indicated here as FEP) are in equilibrium with an equal number of positive and negative charges. Positive charges are induced into one of the electrodes (top or bottom) through contact electrification (when the dielectric layer touches one of the electrodes), creating a difference in the electric potential. The electricity flows as indicated in the panels (in this case from the bottom electrode to the top electrode). When the dielectric layer moves towards the other electrode (in this case the top electrode), owing to the driving force of wind, the process is repeated until the dielectric layer reaches a standstill state. **d**, The turntable-type structure consists of a circular sandwich of the dielectric layer between two bottom electrodes and a top circular electrode (indicated here as Cu foil). In the initial state, the two bottom electrodes have an equal number of positive and negative charges, whereas the top electrode and the dielectric layer have an equal number of positive and negative charges, respectively. The positive charges move between the left and right bottom electrodes following the rotating movement of the top electrodes with the wind force. Al, aluminium; Cu, copper; FEP, fluorinated ethylene propylene.

the output voltage (how much power a device produces to supply the load), the output current (how much current a device can supply to the load) and the output power density (output power of a device divided by its volume). The values of these parameters largely depend on factors such as wind speed, employed materials and power enhancement technologies (such as output power amplification obtained through external amplification systems)[31,76,92]. Regardless of the type of the structure, FEP, PTFE and polyvinyl chloride with Al and Cu electrodes show the best output performances (Fig. 3a). Double-end fixed W-TENGs are more effective in wind energy harvesting.

Hybridization – the combination of W-TENGs with other technologies for power generation – can be used to obtain more effective energy harvesting and expand the application areas[44,45,49,105–108]. For example, having a W-TENG hybridized with an electromagnetic generator can improve the output power from 1.8 mW (for the single electromagnetic generator) to 5 mW (for the hybrid structure)[105]. Other strategies to improve the device performance are charge excitation[87], charge handling[76] and the use of composite membranes[73,109]. Injecting charges into the external circuit can be used to enhance the surface charge density, increasing the number of charge transfers from one electrode to the other, resulting in higher current output[31]. To the same purpose, extra charge injecting pump-TENG[76] and composite materials[73] have been proposed. By applying new materials and using external circuits to increase the device outputs, the performance can be further increased[92,97]. For example, using Ag nanoparticle-based electrodes can produce a pulse current up to 100 mA when a transformer and a power management circuit are used[92]. A disk-shaped turntable W-TENG fabricated using natural cotton can produce a peak output voltage of 782 V and a power output of 1.89 mW (ref. 97).

Another important factor to consider is the influence of the wind speed on the ability of the devices to generate electrical energy (Fig. 3b,c). Different sources such as natural wind, human movement and mechanical residual wind (such as waste wind from industrial machinery) have different speed ranges[68,77]. Natural wind flows depend on temperature and pressure differences and their speed ranges are strongly influenced by factors such as geographical location, topography and season[1,96]. Airflow can also be obtained through human activities, such as breathing or running, which are too weak to be harvested through conventional technologies (speeds usually below 10 m s^{-1})[67,68]. Another large source of wind energy is the airflow (speed ranges from a gentle breeze to high-speed wind) caused by trains, cars and air conditioners[22,39]. Last-generation W-TENGs show high outputs in terms of voltage and current at low-speed wind.

Performance improvement over the years

Since their first introduction, W-TENGs have shown advancement in their design, device output, device stability and range of applications. Since 2013, in over a decade, the output power from a single W-TENG has increased to hundred times from 0.16 mW to the 10 mW range[22,40] (towards 20 mW, Fig. 3d). W-TENGs can now power up to 3,000 LEDs with increasing applications ranging from small sensors to IoT devices, including wireless data transfer[51,70,77]. In 2016, harvesting energy from high-altitude wind (17–22 km) characterized by arbitrary direction was demonstrated[79]. The first hybridization of W-TENG with solar cells was introduced in 2016 (ref. 110). The use of silver nanoparticles for the electrodes to improve the surface charge density was investigated in the same year[92]. In 2020, a W-TENG that can harvest the extremely low wind speed of 0.7 m s^{-1} with an excellent output compared with other high wind speed-driven W-TENGs was proposed[23]. In 2019, a flutter-based W-TENG with an output power range of around 4 mW and the ability to light on more than 100 LEDs was demonstrated[111]. From 2021, the output performances have increased markedly to double digit around 10 mW and the ability to light on almost 500 LEDs[112]. In 2023, optimized power circuitry and the introduction of device arrays have taken the device performances far ahead[22,31,32]. In the first case, a W-TENG is used to collect charges that are transferred to a second W-TENG to increase the charge density at the electrode surface, resulting in output power able to drive a 36-W commercial fluorescent lamp[31]. The array approach works in a similar way: several W-TENGs are stacked together to create an ambient air ionizing channel able to power up 3,000 LEDs[32]. When the airflow (omnidirectional wind) activates the W-TENG, the fluttering dielectric film generates opposite surface charges, which are accumulated in the top and bottom electrodes and are discharged in the ambient air ionizing channel, resulting in a higher number of induced charges on both electrodes and a higher electrical output. In another example, anti-glare panel arrays used on highways showed a power density of 0.2 W m^{-2} and successfully run a radiofrequency identification system[22].

Application areas

The applications of W-TENGs are also continuously evolving. There are two main practical applications of wind energy TENGs: power supply systems and self-powered sensors.

In the first case, wind energy is transformed into electricity, which is stored in energy storage units through circuit management modules[113–115]. This form of W-TENG-based energy supply can be used to supply power to sensors on driverless buses[114,116], for air purification systems[117], in self-powered motion sensors[91,118], water splitting (breakdown of water molecule into hydrogen and oxygen)[119], industrial monitoring[120] and water/oil emulsion separation[101]. W-TENG-based power supply systems can be used to operate smart agricultural sensors[46,103] for insect trapping, soil and ambient humidity detection and temperature detection. Power supplies for various IoT applications have also been introduced: anemometers[121], detectors of water and wind flows for emergency[122], meteorological monitoring[70] and wireless data transfer systems[51,70].

In the second case, W-TENGs can be used as sensors themselves. An external wind produces a specific electrical signal on the W-TENG, which is received by a data collection system for further analysis. The magnitude of the signal (in terms of voltage, current, frequency, capacitance and so on) is measured through signal processing. The obtained data are a measure of the wind speed[50,89,123], wind direction[72], wind level[101,111,122] or any secondary sensing data and can be used to detect vibrations[80,124–126], human motion[68,69] and breathing analysis[127]. More specific applications involve the use of W-TENGs for enhanced metal surface corrosion protection[128], electrochemical degradation[129], high voltage polarization of ferroelectric materials[130], highway anti-glare panels[22], seawater electrolysis[131], wildfire prewarning system[132], cathodic protection[133] and recycling gas energy[134]. W-TENGs are getting more attention as they are favourable in all these applications because of their capability to operate in harsh environments without sacrificing efficiency[135].

Outlook

Energy harvesting through W-TENG technology has the potential to become a widely employed sustainable power source. However, before a large-scale adoption of W-TENGs is possible, some challenges must be addressed.

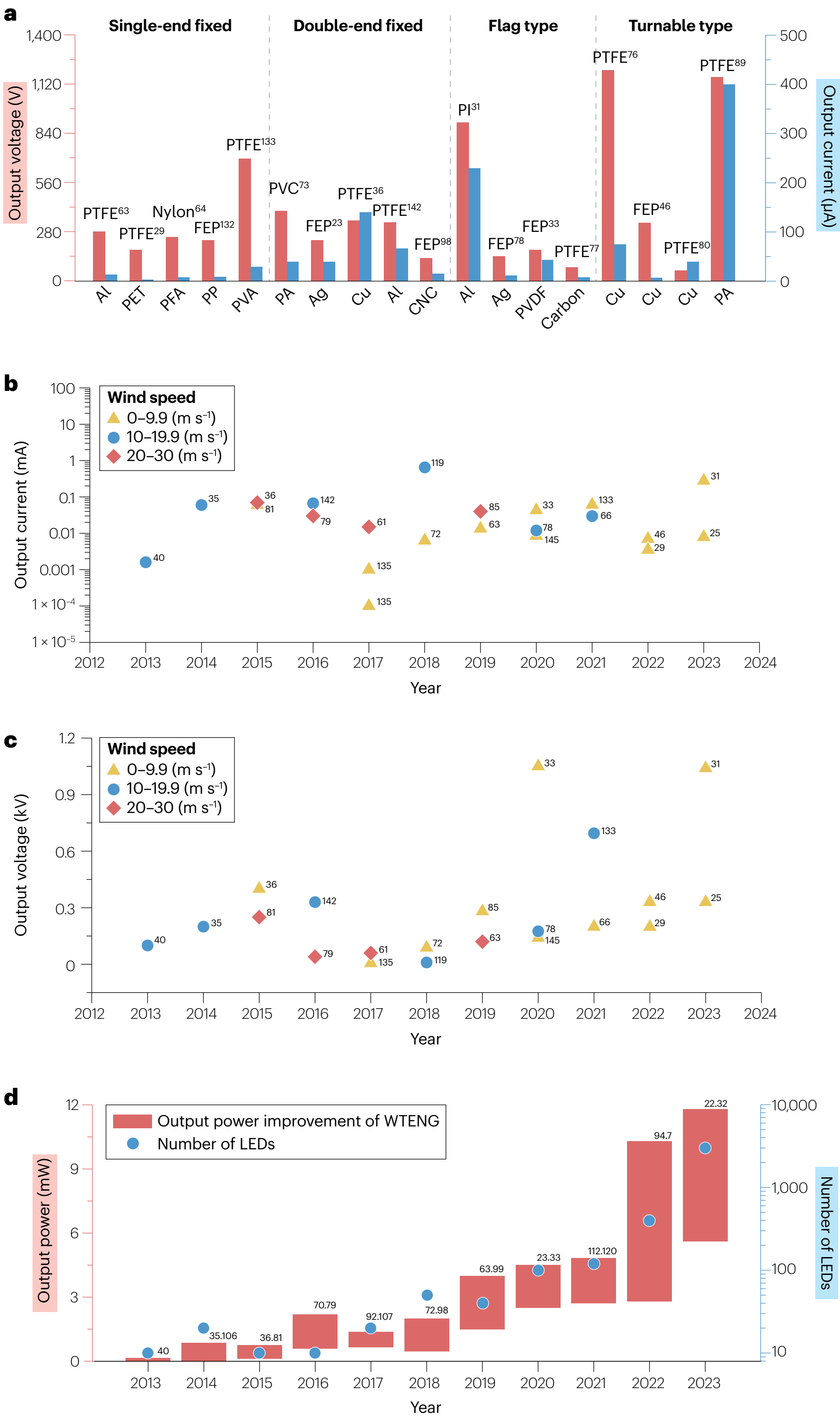

Fig. 3 | Performance of wind-driven triboelectric nanogenerators. a, Output voltages and output currents of wind-driven triboelectric nanogenerator structures fabricated with different materials. Performance evolution over the time of output current (part **b**), output voltage (part **c**) and output power (part **d**). Ag, silver; Al, aluminium; CNC, cellulose nanocrystal; Cu, copper; FEP, fluorinated ethylene propylene; LED, light emitting diode; PA, polyamide; PET, polyethylene terephthalate; PFA, perfluoroalkoxy alkane; PI, polyimide; PP, polypropylene; PTFE, polytetrafluoroethylene; PVA, polyvinyl alcohol; PVC, polyvinyl chloride; PVDF, polyvinylidene fluoride.

The first and most important challenge is the low power outputs of W-TENGs, in comparison to the values from conventional wind turbines. To this aim, device integration and power enhancement techniques can play an important role. Towards industrialization, the scaling up of the device fabrication processes and the synthesis of new materials to improve device lifetime and stability are important points. In addition, it is necessary to evaluate the reliability, stability and lifetime of the devices, through the analysis of the power loss in the transmission process, construction cost and management cost.

W-TENGs have already successfully been deployed in real-life applications in industrial monitoring systems[120], in smart home appliances[136,137], in smart cities[138,139], for air cleaning[140] and for switch automation[141]. Researchers have also demonstrated the integration of W-TENGs into large arrays to simulate large-scale wind farms[109,142]. However, the goal has not yet been achieved[39].

From these examples, it is clear how W-TENG technology is still in its early stages; however, the development of prototypes can trigger industrialization and commercialization. For examples, anti-glare panel arrays used as wind energy harvesters on highways[22], air purification modules[117] and speedometers[22,89,143] have the potential to become the first commercialized products.

There are also special environments with abundant wind energy, such as forests and oceans, where the construction of conventional wind energy generators is not convenient owing to the large size of the blades and the negative environmental impact of the structures. In these environments, wind energy can be harvested using W-TENGs. W-TENGs can sustain extreme meteorological conditions[135] and there are examples of successful hybridization between W-TENG and other energy-scavenging technologies (such as solar panels) that use low wind energy effectively[110,144–146]. Moreover, with the improvement in W-TENG performance, a practical range of applications could be envisioned. Owing to their portability, W-TENGs can be employed in wearable electronics[83,105]. At the same time, replacing batteries with the self-charging mechanisms of W-TENGs is an effective way to reduce potential environmental pollution owing to the massive waste material from batteries.

The underlying fundamental properties and principles should also be investigated to optimize the W-TENG performance. In addition to the application of fundamental knowledge of triboelectricity and dedicated surface engineering, device optimization with the help of computational models and simulation analysis will make the fabrication of the devices effective in less time. So far, in fact, most of the research in W-TENG-based wind energy scavenging is exclusively experimental-oriented, having no simulation counterpart. Developing a computational analysis tool able to implement the cross-relations among working mechanisms, materials, structures, wind speeds and meteorological conditions would permit to study and optimize the device characteristics before the actual fabrication process takes place.

To reach all of these goals, W-TENG technology requires contribution from diverse scientific communities. A cooperative effort from material scientists, physicists and engineers is necessary to make W-TENG technology effectively competitive as a green and clean energy supply with the potential of self-powered portable sensor systems.

Published online: 21 June 2024

References

1. Ang, T. Z. et al. A comprehensive study of renewable energy sources: classifications, challenges and suggestions. *Energy Strategy Rev.* **43**, 100939 (2022).
2. Rathore, M. K. et al. Fabrication and performance analysis of the Aero-leaf Savonius Wind Turbine tree. *Energies* **16**, 3015 (2023).
3. Ayhan, D. & Sağlam, A. A technical review of building-mounted wind power systems and a sample simulation model. *Renew. Sustain. Energy Rev.* **16**, 1040–1049 (2012).
4. Ishugah, T. F., Li, Y., Wang, R. Z. & Kiplagat, J. K. Advances in wind energy resource exploitation in urban environment: a review. *Renew. Sustain. Energy Rev.* **37**, 613–626 (2014).
5. Wahdany, D., Schmitt, C. & Cremer, J. L. More than accuracy: end-to-end wind power forecasting that optimises the energy system. *Electr. Power Syst. Res.* **221**, 109384 (2023).
6. Florescu, A., Barabas, S. & Dobrescu, T. Research on increasing the performance of wind power plants for sustainable development. *Sustainability* **11**, 1266 (2019).
7. Tan, D. et al. Anti-overturning fully symmetrical triboelectric nanogenerator based on an elliptic cylindrical structure for all-weather blue energy harvesting. *Nanomicro Lett.* **14**, 124 (2022).
8. Hutchinson, M. *Global Wind Report* 2023. https://gwec.net/wp-content/uploads/2023/03/GWR-2023_interactive_v2_compressed.pdf (Global Wind Energy Council, 2023).
9. Porté-Agel, F., Bastankhah, M. & Shamsoddin, S. Wind-turbine and wind-farm flows: a review. *Bound. Layer Meteorol.* **174**, 1–59 (2020).
10. Barooni, M., Ashuri, T., Velioglu Sogut, D., Wood, S. & Ghaderpour Taleghani, S. Floating offshore wind turbines: current status and future prospects. *Energies* **16**, 2 (2023).
11. Cherubini, A., Papini, A., Vertechy, R. & Fontana, M. Airborne wind energy systems: a review of the technologies. *Renew. Sustain. Energy Rev.* **51**, 1461–1476 (2015).
12. Shadman, M. et al. A review of offshore renewable energy in South America: current status and future perspectives. *Sustainability* **15**, 1740 (2023).
13. Ahmad, I., M'zoughi, F., Aboutalebi, P., Garrido, I. & Garrido, A. J. Fuzzy logic control of an artificial neural network-based floating offshore wind turbine model integrated with four oscillating water columns. *Ocean Eng.* **269**, 113578 (2023).
14. McKenna, R., Ostman, P. & Fichtner, W. Key challenges and prospects for large wind turbines. *Renew. Sustain. Energy Rev.* **53**, 1212–1221 (2016).
15. Wang, J. et al. Risk-averse based optimal operational strategy of grid-connected photovoltaic/wind/battery/diesel hybrid energy system in the electricity/hydrogen markets. *Int. J. Hydrog. Energy* **48**, 4631–4648 (2023).
16. Chen, M., Zhang, F., Zhu, Y., Zhang, K. & Li, Q. A review of fault diagnosis, status prediction, and evaluation technology for wind turbines. *Energies* **16**, 1125 (2023).
17. Wilberforce, T., Olabi, A. G., Sayed, E. T., Alalmi, A. H. & Abdelkareem, M. A. Wind turbine concepts for domestic wind power generation at low wind quality sites. *J. Clean. Prod.* **394**, 136137 (2023).
18. Peng, H., Zhang, H., Fan, Y., Shangguan, L. & Yang, Y. A review of research on wind turbine bearings' failure analysis and fault diagnosis. *Lubricants* **11**, 14 (2023).
19. Verma, A. S. et al. A review of impact loads on composite wind turbine blades: impact threats and classification. *Renew. Sustain. Energy Rev.* **178**, 113261 (2023).
20. Fan, F. R., Tian, Z. Q. & Lin Wang, Z. Flexible triboelectric generator. *Nano Energy* **1**, 328–334 (2012).
21. Wang, Z. L. & Wang, A. C. On the origin of contact-electrification. *Mater. Today* **30**, 34–51 (2019).
22. Su, E. et al. Rationally designed anti-glare panel arrays as highway wind energy harvester. *Adv. Funct. Mater.* **33**, 2214934 (2023).
In this paper, wind energy is captured from moving vehicles on highways with a high power density of 0.2 W m^{-2} at a wind speed of 3 m s^{-1}.
23. Ren, Z. et al. Energy harvesting from breeze wind (0.7–6 m s^{-1}) using ultra-stretchable triboelectric nanogenerator. *Adv. Energy Mater.* **10**, 2001770 (2020).
This work provides an efficient wind energy harvesting at low speed and frequency, achieving an average output of 20 mW m^{-3} with an inlet wind speed of 0.7 m s^{-1}.
24. Gao, T., Zhao, K., Liu, X. & Yang, Y. Implanting a solid Li-ion battery into a triboelectric nanogenerator for simultaneously scavenging and storing wind energy. *Nano Energy* **41**, 210–216 (2017).
25. Li, H. et al. Leaf-Like TENGs for harvesting gentle wind energy at an air velocity as low as 0.2 m s^{-1}. *Adv. Funct. Mater.* **33**, 2212207 (2023).
This work presents a leaf-like triboelectric nanogenerator for harvesting electrical energy from mild wind of 0.2 m s^{-1} with a peak output power of 3.98 mW.
26. Zhang, C. et al. Harvesting wind energy by a triboelectric nanogenerator for an intelligent high-speed train system. *ACS Energy Lett.* **6**, 1490–1499 (2021).
This work studies on harvesting wind energy from high-speed trains, at low costs and high efficiency by reducing friction force, doubling energy-harvesting efficiency and increasing durability.
27. Dai, S. et al. Omnidirectional wind energy harvester for self-powered agro-environmental information sensing. *Nano Energy* **91**, 106686 (2022).
This works illustrates a hydroxyethyl cellulose film-based wind-driven triboelectric nanogenerator for the continuous monitoring of wind vectors.
28. Su, L. et al. Low detection limit and high sensitivity wind speed sensor based on triboelectrification-induced electroluminescence. *Adv. Sci.* **6**, 1901980 (2019).
This work presents a wind speed sensor integrated with a perovskite-based photodetector based on wind-driven triboelectrification-induced electroluminescence.
29. Yuan, S. et al. Scavenging breeze wind energy (1–8.1 m s^{-1}) by minimalist triboelectric nanogenerator based on the wake galloping phenomenon. *Nano Energy* **100**, 107465 (2022).
30. Zou, H. X. et al. A self-regulation strategy for triboelectric nanogenerator and self-powered wind-speed sensor. *Nano Energy* **95**, 106990 (2022).
31. Chung, S. H. et al. Boosting power output of fluttering triboelectric nanogenerator based on charge excitation through multi-utilization of wind. *Nano Energy* **111**, 108389 (2023).
This work illustrates how to use charge excitation to enhance power outputs in futtering triboelectric nanogenerators.
32. Son, J. & Ho et al. Ultrahigh performance, serially stackable, breeze driven triboelectric generator via ambient air ionizing channel. *Adv. Mater.* **35**, 2300283 (2023).
This work presents a charge-polarization-based flutter-driven triboelectric nanogenerator using an ambient air ionizing channel with a peak voltage and output current of 2,000 V and 4 A, respectively.

33. Chen, X. et al. A triboelectric nanogenerator exploiting the Bernoulli effect for scavenging wind energy. *Cell Rep. Phys. Sci.* **1**, 100207 (2020).
34. Xie, L., Zhai, N., Liu, Y., Wen, Z. & Sun, X. Hybrid triboelectric nanogenerators: from energy complementation to integration. *Research* **2021**, 9143762 (2021).
35. Bae, J. et al. Flutter-driven triboelectrification for harvesting wind energy. *Nat. Commun.* **5**, 4929 (2014).
This work used wind-driven triboelectric nanogenerators to deliver power to portable electronic devices in outdoor environments.
36. Wang, S. et al. Elasto-aerodynamics-driven triboelectric nanogenerator for scavenging air-flow energy. *ACS Nano* **9**, 9554–9563 (2015).
37. Guo, H. et al. Airflow-induced triboelectric nanogenerator as a self-powered sensor for detecting humidity and airflow rate. *ACS Appl. Mater. Interfaces* **6**, 17184–17189 (2014).
38. Wang, Z. L. Triboelectric nanogenerators as new energy technology and self-powered sensors — principles, problems and perspectives. *Faraday Discuss.* **176**, 447–458 (2014).
39. Chen, B., Yang, Y. & Wang, Z. L. Scavenging wind energy by triboelectric nanogenerators. *Adv. Energy Mater.* **8**, 1–13 (2018).
40. Yang, Y. et al. Triboelectric nanogenerator for harvesting wind energy and as self-powered wind vector sensor system. *ACS Nano* **7**, 9461–9468 (2013).
41. Xu, L., Hasan, M. A. M., Wu, H. & Yang, Y. Electromagnetic–triboelectric hybridized nanogenerators. *Energies* **14**, 6219 (2021).
42. Hasan, M. A. M., Wang, Y., Bowen, C. R. & Yang, Y. 2D nanomaterials for effective energy scavenging. *Nano-Micro Lett.* **13**, 1–41 (2021).
43. Quan, T., Wang, X., Wang, Z. L. & Yang, Y. Hybridized electromagnetic-triboelectric nanogenerator for a self-powered electronic watch. *ACS Nano* **9**, 12301–12310 (2015).
44. Xie, Y. et al. Rotary triboelectric nanogenerator based on a hybridized mechanism for harvesting wind energy. *ACS Nano* **7**, 7119–7125 (2013).
45. Guo, Y. et al. Harvesting wind energy: a hybridized design of pinwheel by coupling triboelectrification and electromagnetic induction effects. *Nano Energy* **60**, 641–648 (2019).
46. Li, X. et al. Breeze-driven triboelectric nanogenerator for wind energy harvesting and application in smart agriculture. *Appl. Energy* **306**, 117977 (2022).
47. Hu, L. et al. Electromechanical properties of a hybrid broadband wind energy harvester for smart agriculture monitoring in the loess plateau. *Electronics* **12**, 34 (2023).
48. Yang, Ya. *Hybridized and Couple Nanogenerators Design, Performance, and Applications* (Weinheim, 2020).
49. Lu, P. et al. Swing-structured triboelectric–electromagnetic hybridized nanogenerator for breeze wind energy harvesting. *Adv. Mater. Technol.* **6**, 2100496 (2021).
50. Shen, G. et al. An air velocity monitor for coal mine ventilation based on vortex-induced triboelectric nanogenerator. *Sensors* **22**, 4832 (2022).
51. Liu, D. et al. Wind-driven self-powered wireless environmental sensors for internet of things at long distance. *Nano Energy* **73**, 104819 (2020).
52. Ren, Z., Wu, L., Pang, Y., Zhang, W. & Yang, R. Strategies for effectively harvesting wind energy based on triboelectric nanogenerators. *Nano Energy* **100**, 107522 (2022).
53. Sayigh, A. & Milborrow, D. *The Age of Wind Energy Progress and Future Directions from a Global Perspective*. https://link.springer.com/book/10.1007/978-3-030-26446-8 (2020).
54. Zhang, L. et al. Vortex-induced vibration triboelectric nanogenerator for low speed wind energy harvesting. *Nano Energy* **95**, 107029 (2022).
This work presents wind energy harvesting based on vortex-induced vibration.
55. Zhu, W., Hu, C., Bowen, C. R., Wang, Z. L. & Yang, Y. Scavenging low-speed breeze wind energy using a triboelectric nanogenerator installed inside a square variable diameter channel. *Nano Energy* **100**, 107453 (2022).
56. Caduff, M., Huijbregts, M. A. J., Althaus, H. J., Koehler, A. & Hellweg, S. Wind power electricity: the bigger the turbine, the greener the electricity? *Environ. Sci. Technol.* **46**, 4725–4733 (2012).
57. Stehly, T., Duffy, P. & Mulas Hernando, D. *2022 Cost of Wind Energy Review*. https://www.nrel.gov/docs/fy24osti/88335.pdf (2023).
58. Song, W. et al. A novel wind turbine control strategy to maximize load capacity in severe wind conditions. *Energy Rep.* **8**, 7773–7779 (2022).
59. Shin, Y., Cho, S., Han, S. & Jung, G. Y. Omni-directional wind-driven triboelectric nanogenerator with cross-shaped dielectric film. *Nano Converg.* **8**, 25 (2021).
60. Zaw, N. Y. W., Roh, H., Kim, I., Goh, T. S. & Kim, D. Omnidirectional triboelectric nanogenerator operated by weak wind towards a self-powered anemoscope. *Micromachines* **11**, 414 (2020).
61. Phan, H. et al. Aerodynamic and aeroelastic flutters driven triboelectric nanogenerators for harvesting broadband airflow energy. *Nano Energy* **33**, 476–484 (2017).
62. Ye, C. et al. A triboelectric-electromagnetic hybrid nanogenerator with broadband working range for wind energy harvesting and a self-powered wind speed sensor. *ACS Energy Lett.* **6**, 1443–1452 (2021).
63. Hu, J. et al. A flutter-effect-based triboelectric nanogenerator for breeze energy collection from arbitrary directions and self-powered wind speed sensor. *Nano Res.* **12**, 3018–3023 (2019).
64. Tcho, I. W. et al. A flutter-driven triboelectric nanogenerator for harvesting energy of gentle breezes with a rear-fixed fluttering film. *Nano Energy* **98**, 107197 (2022).
65. Fu, X. et al. Breeze-wind-energy-powered autonomous wireless anemometer based on rolling contact-electrification. *ACS Energy Lett.* **6**, 2343–2350 (2021).
66. Zhang, X. et al. Harvesting multidirectional breeze energy and self-powered intelligent fire detection systems based on triboelectric nanogenerator and fluid-dynamic modeling. *Adv. Funct. Mater.* **31**, 2106527 (2021).
67. Xiong, Y. et al. Scalable spinning, winding, and knitting graphene textile TENG for energy harvesting and human motion recognition. *Nano Energy* **107**, 108137 (2023).
68. Zhang, H. et al. Flexible single-electrode triboelectric nanogenerator with MWCNT/PDMS composite film for environmental energy harvesting and human motion monitoring. *Rare Met.* **41**, 3117–3128 (2031).
69. Mao, Y. et al. Nanogenerator-based wireless intelligent motion correction system for storing mechanical energy of human motion. *Sustainability* **14**, 6944 (2022).
70. Zhang, H. et al. Self-powered, wireless, remote meteorologic monitoring based on triboelectric nanogenerator operated by scavenging wind energy. *ACS Appl. Mater. Interfaces* **8**, 32649–32654 (2016).
71. Su, Y. et al. Wind energy harvesting and self-powered flow rate sensor enabled by contact electrification. *J. Phys. D Appl. Phys* **49**, 215601 (2016).
72. Wang, J. et al. Self-powered wind sensor system for detecting wind speed and direction based on a triboelectric nanogenerator. *ACS Nano* **12**, 3954–3963 (2018).
73. Zhao, K. et al. High-performance and long-cycle life of triboelectric nanogenerator using PVC/MoS_2 composite membranes for wind energy scavenging application. *Nano Energy* **91**, 106649 (2022).
74. Chen, X. et al. Boosting output performance of triboelectric nanogenerator via mutual coupling effects enabled photon-carriers and plasmon. *Adv. Sci.* **9**, 2103957 (2022).
75. Wang, Y. et al. A novel humidity resisting and wind direction adapting flag-type triboelectric nanogenerator for wind energy harvesting and speed sensing. *Nano Energy* **78**, 105279 (2020).
76. Yu, X. et al. High-performance triboelectric nanogenerator with synchronization mechanism by charge handling. *Energy Convers. Manag.* **263**, 115655 (2022).
77. Zou, Y. et al. A high-performance flag-type triboelectric nanogenerator for scavenging energy harvesting toward self-powered IoTs. *Materials* **15**, 3696 (2022).
78. Sun, W., Ding, Z., Qin, Z., Chu, F. & Han, Q. Wind energy harvesting based on fluttering double-flag type triboelectric nanogenerators. *Nano Energy* **70**, 104526 (2020).
79. Zhao, Z. et al. Freestanding flag-type triboelectric nanogenerator for harvesting high-altitude wind energy from arbitrary directions. *ACS Nano* **10**, 1780–1787 (2016).
80. Lu, S. et al. Simultaneous energy harvesting and signal sensing from a single triboelectric nanogenerator for intelligent self-powered wireless sensing systems. *Nano Energy* **75**, 104813 (2020).
81. Wang, S. et al. Flow-driven triboelectric generator for directly powering a wireless sensor node. *Adv. Mater.* **27**, 240–248 (2015).
82. Feng, Y. et al. Leaves based triboelectric nanogenerator (TENG) and TENG tree for wind energy harvesting. *Nano Energy* **55**, 260–268 (2019).
83. Wen, Z. et al. Blow-driven triboelectric nanogenerator as an active alcohol breath analyzer. *Nano Energy* **16**, 38–46 (2015).
84. Heo, Y. G. et al. Ventilator integrated triboelectric nanogenerator based on structure of centrifugal brake. *Surf. Interfaces* **27**, 101525 (2021).
85. Lin, H. et al. Angle-shaped triboelectric nanogenerator for harvesting environmental wind energy. *Nano Energy* **56**, 269–276 (2019).
86. Liu, W. et al. Integrated charge excitation triboelectric nanogenerator. *Nat. Commun.* **10**, 1–9 (2019).
87. Liu, Y. et al. Quantifying contact status and the air-breakdown model of charge-excitation triboelectric nanogenerators to maximize charge density. *Nat. Commun.* **11**, 1599 (2020).
88. Yang, Z. et al. Charge pumping for sliding-mode triboelectric nanogenerator with voltage stabilization and boosted current. *Adv. Energy Mater.* **11**, 2101147 (2021).
89. He, L. et al. A dual-mode triboelectric nanogenerator for wind energy harvesting and self-powered wind speed monitoring. *ACS Nano* **16**, 6244–6254 (2022).
90. Ko, H. J., Kwon, D. S., Bae, K. & Kim, J. Self-suspended shell-based triboelectric nanogenerator for omnidirectional wind-energy harvesting. *Nano Energy* **96**, 107062 (2022).
91. Yi, F. et al. Stretchable-rubber-based triboelectric nanogenerator and its application as self-powered body motion sensors. *Adv. Funct. Mater.* **25**, 3688–3696 (2015).
92. Jiang, Q., Chen, B., Zhang, K. & Yang, Y. Ag nanoparticle-based triboelectric nanogenerator to scavenge wind energy for a self-charging power unit. *ACS Appl. Mater. Interfaces* **9**, 43716–43723 (2017).
93. Cho, H., Jo, S., Kim, I. & Kim, D. Film-sponge-coupled triboelectric nanogenerator with enhanced contact area based on direct ultraviolet laser ablation. *ACS Appl. Mater. Interfaces* **13**, 48281–48291 (2021).
94. Kinas, Z. et al. High-performance triboelectric nanogenerator based on carbon nanomaterials functionalized polyacrylonitrile nanofibers. *Energy* **239**, 122369 (2022).
95. Minhas, J. Z., Hasan, M. A. M. & Yang, Y. Ferroelectric materials based coupled nanogenerators. *Nanoenergy Adv.* **1**, 131–180 (2021).
96. Tan, J. D., Chang, C. C. W., Bhuiyan, M. A. S., Minhad, K. N. & Ali, K. Advancements of wind energy conversion systems for low-wind urban environments: a review. *Energy Rep.* **8**, 3406–3414 (2022).
97. Xia, R. et al. Natural cotton-based triboelectric nanogenerator as a self-powered system for efficient use of water and wind energy. *Nano Energy* **92**, 106685 (2022).
98. Chen, B., Yang, N., Jiang, Q., Chen, W. & Yang, Y. Transparent triboelectric nanogenerator-induced high voltage pulsed electric field for a self-powered handheld printer. *Nano Energy* **44**, 468–475 (2018).
99. Ravichandran, A. N., Calmes, C., Serres, J. R., Ramuz, M. & Blayac, S. Compact and high performance wind actuated venturi triboelectric energy harvester. *Nano Energy* **62**, 449–457 (2019).

100. Yuan You, Z. et al. An organic semiconductor/metal Schottky heterojunction based direct current triboelectric nanogenerator windmill for wind energy harvesting. *Nano Energy* **109**, 108302 (2023).
101. Li, X. et al. Carbon nano thorn arrays based water/cold resisted nanogenerator for wind energy harvesting and speed sensing. *Nano Energy* **90**, 106571 (2021).
102. Yong, H. et al. Highly reliable wind-rolling triboelectric nanogenerator operating in a wide wind speed range. *Sci. Rep.* **6**, 33977 (2016).
103. Han, J. et al. Wind-driven soft-contact rotary triboelectric nanogenerator based on rabbit fur with high performance and durability for smart farming. *Adv. Funct. Mater.* **32**, 2108580 (2022).
104. Zheng, N., Xue, J., Jie, Y., Cao, X. & Wang, Z. L. Wearable and humidity-resistant biomaterials-based triboelectric nanogenerator for high entropy energy harvesting and self-powered sensing. *Nano Res.* **15**, 6213–6219 (2022).
105. Wang, X., Wang, S., Yang, Y. & Wang, Z. L. Hybridized electromagnetic–triboelectric nanogenerator for scavenging air-flow energy to sustainably power temperature sensors. *ACS Nano* **9**, 4553–4562 (2015).
106. Wu, Y., Zhong, X., Wang, X., Yang, Y. & Wang, Z. L. Hybrid energy cell for simultaneously harvesting wind, solar, and chemical energies. *Nano Res.* **7**, 1631–1639 (2014).
107. Wang, J. et al. Smart network node based on hybrid nanogenerator for self-powered multifunctional sensing. *Nano Energy* **33**, 418–426 (2017).
108. Rahman, M. T. et al. Natural wind-driven ultra-compact and highly efficient hybridized nanogenerator for self-sustained wireless environmental monitoring system. *Nano Energy* **57**, 256–268 (2019).
This work discusses the hybridization of an electromagnetic generator with a piezoelectric nanogenerator and a triboelectric nanogenerator.
109. Dudem, B. et al. Nanopillar-array architectured PDMS-based triboelectric nanogenerator integrated with a windmill model for effective wind energy harvesting. *Nano Energy* **42**, 269–281 (2017).
110. Dudem, B., Ko, Y. H., Leem, J. W., Lim, J. H. & Yu, J. S. Hybrid energy cell with hierarchical nano/micro-architectured polymer film to harvest mechanical, solar, and wind energies individually/simultaneously. *ACS Appl. Mater. Interfaces* **8**, 30165–30175 (2016).
111. Olsen, M. et al. Frequency and voltage response of a wind-driven fluttering triboelectric nanogenerator. *Sci. Rep.* **9**, 5543 (2019).
112. Liu, S. et al. Magnetic switch structured triboelectric nanogenerator for continuous and regular harvesting of wind energy. *Nano Energy* **83**, 105851 (2021).
113. Tang, X. et al. Self-powered wind sensor based on triboelectric nanogenerator for detecting breeze vibration on electric transmission lines. *Nano Energy* **99**, 107412 (2022).
114. Tang, M. et al. A hybrid kinetic energy harvester for applications in electric driverless buses. *Int. J. Mech. Sci.* **223**, 107317 (2022).
115. Yang, D. et al. An asymmetric AC electric field of triboelectric nanogenerator for efficient water/oil emulsion separation. *Nano Energy* **90**, 106641 (2021).
116. Xu, Y. et al. Real-time monitoring system of automobile driver status and intelligent fatigue warning based on triboelectric nanogenerator. *ACS Nano* **15**, 7271–7278 (2021).
117. Li, C. L. et al. A self-priming air filtration system based on triboelectric nanogenerator for active air purification. *Chem. Eng. J.* **452**, 139428 (2023).
118. Sukumaran, C., Viswanathan, P., Munirathinam, P. & Chandrasekhar, A. A flexible and wearable joint motion sensor using triboelectric nanogenerators for hand gesture monitoring. *Int. J. Nanotechnol.* **18**, 697–704 (2017).
119. Ren, X. et al. Wind energy harvester based on coaxial rotatory freestanding triboelectric nanogenerators for self-powered water splitting. *Nano Energy* **50**, 562–570 (2018).
This work introduces a water splitting process powered by wind-driven triboelectric nanogenarator.
120. Zhang, J. et al. Irregular wind energy harvesting by a turbine vent triboelectric nanogenerator and its application in a self-powered on-site industrial monitoring system. *ACS Appl. Mater. Interfaces* **13**, 55136–55144 (2021).
121. Fang, Y. et al. A high-performance triboelectric-electromagnetic hybrid wind energy harvester based on rotational tapered rollers aiming at outdoor IoT applications. *iScience* **24**, 102300 (2021).
122. Zhang, Q. et al. Self-sustainable flow-velocity detection via electromagnetic/triboelectric hybrid generator aiming at IoT-based environment monitoring. *Nano Energy* **90**, 106501 (2021).
123. Liu, Y., Liu, J. & Che, L. A high sensitivity self-powered wind speed sensor based on triboelectric nanogenerators (TENGs). *Sensors* **21**, 2951 (2021).
124. Zeng, Q. et al. A high-efficient breeze energy harvester utilizing a full-packaged triboelectric nanogenerator based on flow-induced vibration. *Nano Energy* **70**, 104524 (2020).
125. Chen, J. & Wang, Z. L. Reviving vibration energy harvesting and self-powered sensing by a triboelectric nanogenerator. *Joule* **1**, 480–521 (2017).
126. Ren, Z., Wang, Z., Wang, F., Li, S. & Wang, Z. L. Vibration behavior and excitation mechanism of ultra-stretchable triboelectric nanogenerator for wind energy harvesting. *Extreme Mech. Lett.* **45**, 101285 (2021).
This work investigates the correlation between vibration and excitation mechanism for wind energy harvesting by using computational fluid dynamics and aerodynamic models.
127. Yum, H. Y., Han, S. A., Konstantinov, K., Kim, S. W. & Kim, J. H. Smart triboelectric nanogenerators toward human-oriented technologies: health monitoring, wound healing, drug delivery. *Adv. Mater. Technol.* **8**, 2201500 (2023).
128. Zhu, H. R. et al. Self-powered metal surface anti-corrosion protection using energy harvested from rain drops and wind. *Nano Energy* **14**, 193–200 (2014).
129. Liu, L. et al. Improved degradation efficiency of levofloxacin by a self-powered electrochemical system with pulsed direct-current. *ACS Nano* **15**, 5478–5485 (2021).
130. Liu, X., Zhao, K. & Yang, Y. Effective polarization of ferroelectric materials by using a triboelectric nanogenerator to scavenge wind energy. *Nano Energy* **53**, 622–629 (2018).
This work demonstrates the effective polarization of ferroelectric materials by using wind-driven triboelectric nanogenerators.
131. Zhu, Z. et al. Continuously harvesting energy from water and wind by pulsed triboelectric nanogenerator for self-powered seawater electrolysis. *Nano Energy* **93**, 106776 (2022).
132. Gao, X. et al. A turbine disk-type triboelectric nanogenerator for wind energy harvesting and self-powered wildfire pre-warning. *Mater. Today Energy* **22**, 100867 (2021).
133. Sun, W. et al. Humidity-resistant triboelectric nanogenerator and its applications in wind energy harvesting and self-powered cathodic protection. *Electrochim. Acta* **391**, 138994 (2021).
134. Ma, M. et al. Integrated hybrid nanogenerator for gas energy recycle and purification. *Nano Energy* **39**, 524–531 (2017).
135. Xu, M. et al. An aeroelastic flutter based triboelectric nanogenerator as a self-powered active wind speed sensor in harsh environment. *Extreme Mech. Lett.* **15**, 122–129 (2017).
136. Rana, S. M. S. et al. Electrospun PVDF-TrFE/MXene nanofiber mat-based triboelectric nanogenerator for smart home appliances. *ACS Appl. Mater. Interfaces* **13**, 4955–4967 (2021).
137. Zhang, L. et al. Lawn structured triboelectric nanogenerators for scavenging sweeping wind energy on rooftops. *Adv. Mater.* **28**, 1650–1656 (2016).
This work presents a wind-driven triboelectric nanogerator with an optimized surface nanostructure.
138. Alagumalai, A. et al. Towards smart cities powered by nanogenerators: bibliometric and machine learning-based analysis. *Nano Energy* **83**, 105844 (2021).
139. Liu, L., Guo, X. & Lee, C. Promoting smart cities into the 5G era with multi-field Internet of Things (IoT) applications powered with advanced mechanical energy harvesters. *Nano Energy* **88**, 106304 (2021).
140. Chen, S. et al. Self-powered cleaning of air pollution by wind driven triboelectric nanogenerator. *Nano Energy* **14**, 217–225 (2014).
141. Yong, S. et al. Auto-switching self-powered system for efficient broad-band wind energy harvesting based on dual-rotation shaft triboelectric nanogenerator. *Adv. Energy Mater.* **11**, 2101194 (2021).
142. Quan, Z., Han, C. B., Jiang, T. & Wang, Z. L. Robust thin films-based triboelectric nanogenerator arrays for harvesting bidirectional wind energy. *Adv. Energy Mater.* **6**, 1501799 (2016).
143. Qin, Q., Cao, X. & Wang, N. Ball-mill-inspired durable triboelectric nanogenerator for wind energy collecting and speed monitoring. *Nanomaterials* **13**, 939 (2023).
144. Xu, G. P. et al. A triboelectric/electromagnetic hybrid generator for efficient wind energy collection and power supply for electronic devices. *Sci. China Technol. Sci.* **64**, 2003–2011 (2021).
145. Zhang, Y. et al. An ultra-durable windmill-like hybrid nanogenerator for steady and efficient harvesting of low-speed wind energy. *Nanomicro Lett.* **12**, 1–11 (2020).
146. Wang, P. et al. An ultra-low-friction triboelectric-electromagnetic hybrid nanogenerator for rotation energy harvesting and self-powered wind speed sensor. *ACS Nano* **12**, 9433–9440 (2018).
147. Marti-Puig, P., Blanco-M, A., Cusidó, J. & Solé-Casals, J. Wind turbine database for intelligent operation and maintenance strategies. *Sci. Data* **11**, 255 (2024).
148. Seol, M. L. et al. Vertically stacked thin triboelectric nanogenerator for wind energy harvesting. *Nano Energy* **14**, 201–208 (2015).
149. Pathak, S. et al. Ultra-low friction self-levitating nanomagnetic fluid bearing for highly efficient wind energy harvesting. *Sustain. Energy Technol. Assess.* **52**, 102024 (2022).
150. Settar Subry Kerearn, E., Mohammed, K. G., Sahib, M., Kerearn, S. S. & Sahib Ibrahim, M. Analysis study in principles of operation Of DC machine. *J. Adv. Res. Dyn. Control. Syst.* **10**, 2323–2329 (2018).
151. Macangus-Gerrard, G. Alternating current synchronous generators. in *Offshore Electrical Engineering Manual* 35–42 (Elsevier, 2018).
152. Su, Y. et al. Segmented wind energy harvester based on contact-electrification and as a self-powered flow rate sensor. *Chem. Phys. Lett.* **653**, 96–100 (2016).
153. Lin, Z. H., Cheng, G., Lee, S., Pradel, K. C. & Wang, Z. L. Harvesting water drop energy by a sequential contact-electrification and electrostatic-induction process. *Adv. Mater.* **26**, 4690–4696 (2014).

Acknowledgements
This work was supported by the National Key R & D Project from the Ministry of Science and Technology in China (no. 2021YFA1201604), the National Natural Science Foundation of China (grant no. 52072041), the Beijing Natural Science Foundation (grant no. JQ21007) and the ANSO (Alliance of International Science Organizations).

Author contributions

M.A.M.H. and W.Z. surveyed literature, collected and researched data for the article. M.A.M.H., W.Z. and Y.Y. contributed substantially to the discussion of the content. M.A.M.H., W.Z. and Y.Y. wrote the article. C.R.B., Z.L.W. and Y.Y. reviewed and edited the manuscript before submission.

Competing interests

The authors declare no competing interests.

Additional information

Peer review information *Nature Reviews Electrical Engineering* thanks Arunkumar Chandrasekhar, Alberto Vomiero and Weiqiang Zhang for their contribution to the peer review of this work.